

Physics-Driven Dual-Defect Model Fits of Voltage Step-Up to Breakdown Data in Spacecraft Polymers

Allen Andersen

Jet Propulsion Laboratory, California Institute of Technology
4800 Oak Grove Dr., Mail Stop 156-206
Pasadena, CA 91109 USA
allen.j.andersen@jpl.nasa.gov

JR Dennison

Materials Physics Group
Utah State University
4415 Old Main Hill, Logan, UT 84322 USA
jr.dennison@usu.edu

Abstract—Overly conservative estimates of breakdown strength can increase the mass and cost of spacecraft electrostatic discharge (ESD) mitigation methods. Improved estimates of ESD likelihood in the space environment require better models of ESD distributions. The purpose of this work is to evaluate our previously proposed dual-defect model of voltage step-up-to-breakdown tests with a case study across four dielectric materials. We predicted that materials best fit by mixed Weibull distributions would exhibit better fits with the dual-defect model compared to a mean field single defect theory. Additional data for biaxially oriented polypropylene (BOPP), polyimide (PI or Kapton) from three sources, and polyether ether ketone (PEEK) are compared to the previous study on low-density polyethylene (LDPE). Except in one case, the dual-defect model is a better fit to bimodal distributions of tests results.

I. INTRODUCTION

Spacecraft in the space plasma environment accumulate charge over time and the lack of electrical ground together with low charge mobility in some spacecraft materials can cause electric fields to build up—potentially leading catastrophic electrostatic discharge (ESD) events. These ESDs are the primary cause for spacecraft failures and anomalies from interactions with the space environment [1-4].

Spacecraft charging mitigation guidelines often give rule-of-thumb values for ESD threshold fields ranging from 1 to 20 MV/m [4-7]. Given the worst case space radiation environment—often with some added safety margin—together with a material’s dark and radiation induced conductivity, one can model potentials in a dielectric with software tools such as NUMIT [8]. If the modeled potential reaches the ESD threshold field, then a significant risk of discharge is predicted. Designers must then, by test or analysis, assess if this source of ESD may couple into any sensitive components.

This simplified perspective ignores the fact that the likelihood of ESD occurrence at a given field may vary significantly from material to material [9]. Such unquantified conservatism can come at the cost of excessive shielding mass or prohibitive dielectric thickness design constraints. In the case of potential lander missions to Jovian icy moons, dielectrics will be subjected to intense radiation without respite at cold temperatures for the duration of its surface operations. In such conditions it is very unlikely for reasonable spacecraft designs to maintain electric fields below rule-of-thumb ESD thresholds for the duration of the mission. Improved understanding of

conduction and ESD properties of dielectric materials will be key to the success of such missions.

In a previous publication, we proposed that ESD distributions best fit by mixed Weibull distributions are indicative of dual-defect mechanisms contributing to breakdown [10]. This notion was drawn from ESD tests on low-density polyethylene (LDPE). In this paper we present fits to the empirical cumulative distribution (ECD) of the room temperature voltage step-up ESD tests of biaxially-oriented polypropylene (BOPP), three batches of polyimide (PI), and polyether ether ketone (PEEK) to Weibull distributions and our physics based dual-defect model. Extensive experimental and theoretical details are given in other publications [11, 12].

II. Dual-Defect Models

The dual-defect model we propose can be derived from runaway thermally assisted hopping between electron defects or trap states. This model is an extension of Crine’s mean field theory—which is equivalent to a model with a single average defect density and energy [13]. The dual defect model assumes that both shallow (lower energy) physical defects and deep (higher energy) chemical defects contribute to breakdown, represented as the sum of mean shallow and mean deep defect energy and density contributions [11, 14]. Applied to the voltage step-up test problem, this model is expressed as

$$P_{step}^{Tot} = 1 - \prod_{j=1}^{N_{step}} \left[1 - P_{def}^{Tot} \left(\Delta t_{step}, \frac{j \Delta V_{step}}{d}, T \right) \right] \quad (1)$$

where

$$\begin{aligned} P_{def}^{Tot} &= \sum_{i=HI,LO} P_{def}^i \\ &= \left(\frac{2k_b T}{h/\Delta t} \right) \sum_{i=HI,LO} \exp \left[\frac{-\Delta G_{def}^i}{k_b T} \right] \sinh \left[\frac{\epsilon_0 \epsilon_r F^2}{2N_{def}^i k_b T} \right] \end{aligned} \quad (2)$$

The details of this theory are not presented here due to length constraints, but are given in detail in [11]. The key intrinsic material parameters are two defect (trap) energies ΔG_{def}^i and two densities N_{def}^i for $i = HI$ (deep) and $i = LO$ (shallow) type defects. Like Weibull distributions, Eq. (2) predicts the likelihood of breakdown as a function of electric field, but the fitting parameters have explicit physical interpretations at the expense of added complexity. For a single defect species, Eq. (1) reduces to the Crine model [13].

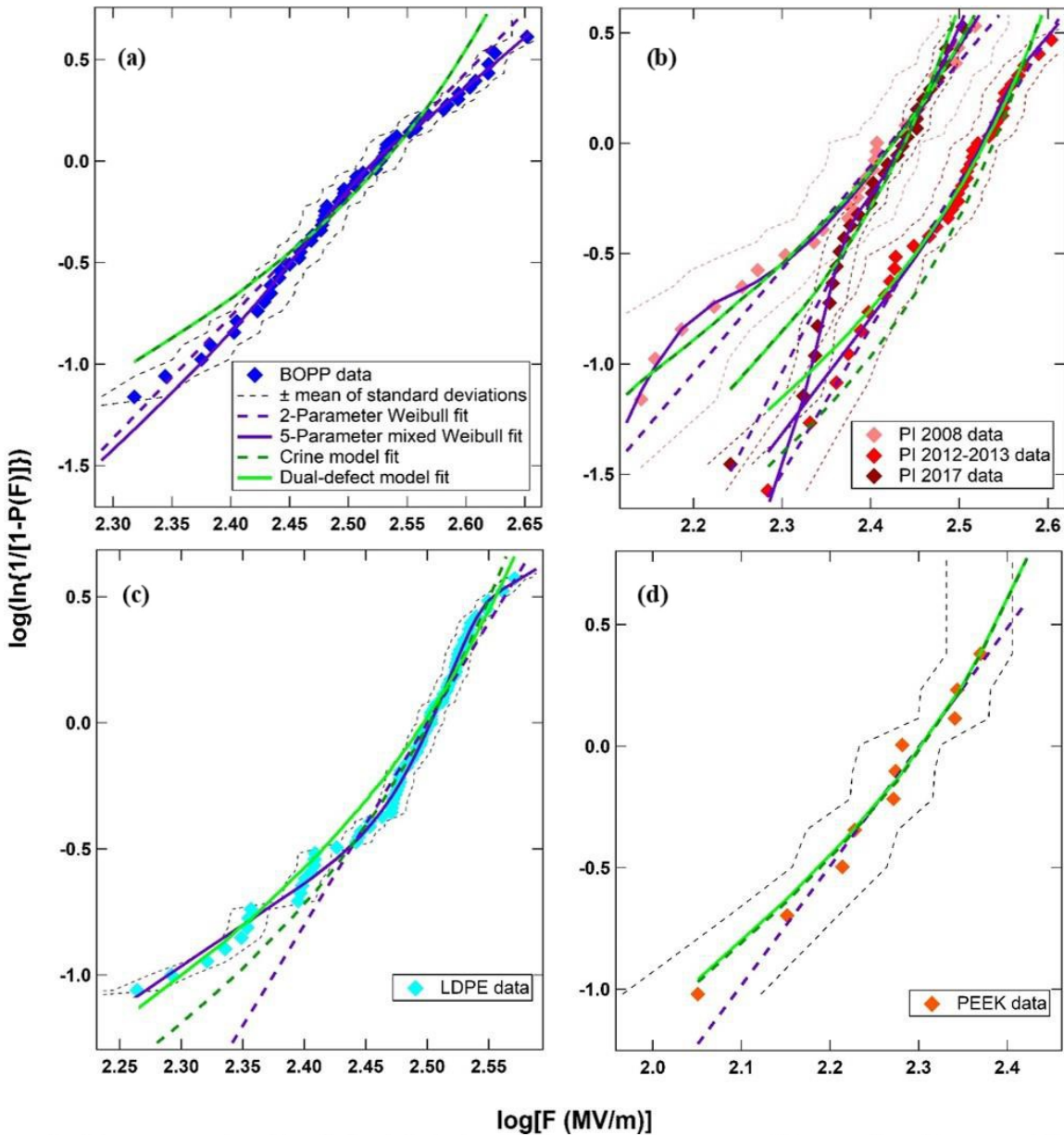


FIG. 1. Step-up to breakdown tests together with Weibull and physics-based fits for room temperature tests of (a) BOPP, (b) PI, (c) LDPE, and (d) PEEK. In each case the better of the 2- or 5-parameter Weibull fit (see Table 1) is shown. Estimates of the uncertainties in measured values as the mean of the standard deviations are shown as dashed lines about the fits.

Figure 1 and Table 1 show the results of fits with single and mixed-Weibull functions and single- and dual-defect physics models, where the Weibull parameters are the field corresponding to a 63.2% probability of breakdown F_0 , and a width parameter β . Incorporating an inception field into a Weibull distribution requires a third parameter, F_S . The mixture of two 2-parameter Weibull functions contains p for the fractional weight of the first two-parameter Weibull distribution; F_{01} and F_{02} are their distribution centroids, and β_1 and β_2 are the corresponding width parameters.

III. Discussion of Fits to Breakdown Data

With Weibull fits for different materials, or even different batches of nominally the same material, we can begin to make comparisons. Batches of PI measured in 2008 and 2017 have very similar breakdown voltages, but the much lower shape parameter for the 2008 batch indicates a greater likelihood of breakdown at lower voltages. We see that for BOPP and PI 2012-2013 data a threshold field for breakdown F_S can be clearly defined. For PEEK, which had only 11 tests, anything more complicated than a two-parameter Weibull is an exercise in futility; there simply are not enough data to justify more

TABLE I
Comparison of Weibull, Crine, and Dual-defect Model Fits to Voltage Step-up Tests

Material	2-parameter Weibull function	3-parameter Weibull function	5-parameter Weibull function	Crine model	Dual-defect model
BOPP	$F_0 = 337.0 \pm 0.8$ MV/m $\beta = 6.0 \pm 0.1$	$F_0 = 335.7 \pm 0.7$ MV/m $\beta = 2.9 \pm 0.3$ $F_3 = 170 \pm 10$ MV/m	$F_{01} = 309 \pm 2$ MV/m $F_{02} = 349 \pm 3$ MV/m $\beta_1 = 13 \pm 2$ $\beta_2 = 5.4 \pm 0.2$ $p = 0.24 \pm 0.05$	$\Delta G_{def} = 0.99 \pm 0.01$ eV $N_{def} = (8.2 \pm 0.3) \cdot 10^{19} \text{cm}^{-3}$	$\Delta G_{def}^{HI} = 1.1$ eV $\Delta G_{def}^{LO} = 1.0$ eV $N_{def}^{HI} = 8.1 \cdot 10^{19} \text{cm}^{-3}$ $N_{def}^{LO} = 8.2 \cdot 10^{19} \text{cm}^{-3}$
PI 2008	$F_0 = 264 \pm 1$ MV/m $\beta = 4.7 \pm 0.2$	$F_0 = 264 \pm 2$ MV/m $\beta = 5 \pm 2$ $F_3 = 0 \pm 90$ MV/m	$F_{01} = 146 \pm 7$ MV/m $F_{02} = 273 \pm 2$ MV/m $\beta_1 = 10 \pm 8$ $\beta_2 = 6.5 \pm 0.4$ $p = 0.14 \pm 0.03$	$\Delta G_{def} = 1.0 \pm 0.1$ eV $N_{def} = (9.1 \pm 0.4) \cdot 10^{19} \text{cm}^{-3}$	$\Delta G_{def}^{HI} = 1.1$ eV $\Delta G_{def}^{LO} = 1 \pm 2$ eV $N_{def}^{HI} = 7.1 \cdot 10^{19} \text{cm}^{-3}$ $N_{def}^{LO} = (9 \pm 9) \cdot 10^{19} \text{cm}^{-3}$
PI 2012-2013	$F_0 = 336.3 \pm 0.9$ MV/m $\beta = 6.6 \pm 0.2$	$F_0 = 336 \pm 1$ MV/m $\beta = 7 \pm 3$ $F_3 = 0 \pm 100$ MV/m	$F_{01} = 330 \pm 5$ MV/m $F_{02} = 344 \pm 5$ MV/m $\beta_1 = 5.3 \pm 0.8$ $\beta_2 = 16 \pm 8$ $p = 0.74 \pm 0.2$	$\Delta G_{def} = 1$ eV $N_{def} = 1 \cdot 10^{20} \text{cm}^{-3}$	$\Delta G_{def}^{HI} = 1.03$ eV $\Delta G_{def}^{LO} = 1.02$ eV $N_{def}^{HI} = 1.3 \cdot 10^{20} \text{cm}^{-3}$ $N_{def}^{LO} = 1.2 \cdot 10^{20} \text{cm}^{-3}$
PI 2017	$F_0 = 272.3 \pm 0.8$ MV/m $\beta = 7.7 \pm 0.2$	$F_0 = 271.1 \pm 0.9$ MV/m $\beta = 3.2 \pm 0.7$ $F_3 = 150 \pm 20$ MV/m	$F_{01} = 230 \pm 1$ MV/m $F_{02} = 282 \pm 2$ MV/m $\beta_1 = 25 \pm 6$ $\beta_2 = 10 \pm 1$ $p = 0.23 \pm 0.05$	$\Delta G_{def} = 1$ eV $N_{def} = 6 \cdot 10^{19} \text{cm}^{-3}$	$\Delta G_{def}^{HI} = 1.04$ eV $\Delta G_{def}^{LO} = 1.02$ eV $N_{def}^{HI} = 6.5 \cdot 10^{19} \text{cm}^{-3}$ $N_{def}^{LO} = 6.4 \cdot 10^{19} \text{cm}^{-3}$
LDPE	$F_0 = 316.4 \pm 0.7$ MV/m $\beta = 4.7 \pm 0.2$	$F_0 = 316.4 \pm 0.8$ MV/m $\beta = 8 \pm 4$ $F_3 = 0 \pm 200$ MV/m	$F_{01} = 282 \pm 7$ MV/m $F_{02} = 323.8 \pm 0.8$ MV/m $\beta_1 = 3.6 \pm 0.3$ $\beta_2 = 17 \pm 1$ $p = 0.41 \pm 0.04$	$\Delta G_{def} = 1.02 \pm 0.08$ eV $N_{def} = (4.39 \pm 0.09) \cdot 10^{19} \text{cm}^{-3}$	$\Delta G_{def}^{HI} = 1.06$ eV $\Delta G_{def}^{LO} = 1.0 \pm 0.2$ eV $N_{def}^{HI} = 9.3 \cdot 10^{24} \text{cm}^{-3}$ $N_{def}^{LO} = (3.8 \pm 0.2) \cdot 10^{19} \text{cm}^{-3}$
PEEK	$F_0 = 200 \pm 2$ MV/m $\beta = 4.9 \pm 0.4$	$F_0 = 200 \pm 2$ MV/m $\beta = 10 \pm 10$ $F_3 = 0 \pm 400$ MV/m	$F_{01} = 0 \pm 5000$ MV/m $F_{02} = 0 \pm 2000$ MV/m $\beta_1 = 0 \pm 50$ $\beta_2 = 0 \pm 50$ $p = 0 \pm 100$	$\Delta G_{def} = 1$ eV $N_{def} = 5 \cdot 10^{19} \text{cm}^{-3}$	$\Delta G_{def}^{HI} = 1.09$ eV $\Delta G_{def}^{LO} = 0.96$ eV $N_{def}^{HI} = 1.5 \cdot 10^{22} \text{cm}^{-3}$ $N_{def}^{LO} = 4.8 \cdot 10^{19} \text{cm}^{-3}$

complex fits. Note that the ASTM standard for dc breakdown testing recommends a minimum of only five tests [15]. Excepting cursory material comparisons, this seems woefully inadequate.

Uncertainties are only listed for parameters where the resulting uncertainties were not much larger than the parameters themselves. For such fits, *Igor Pro* fitting routines used here still yielded repeatable results, even without complete fit convergence after a limited number of iterations. We first note that all results fall into the realm of physically reasonable results based on the range of realistic energies and densities discussed. While the results are all near 1 eV and 10^{20}cm^{-3} , recall that even a few times the thermal energy $k_b T$ at room temperature (~ 0.03 eV) represent significant differences in transition probabilities and therefore the results show significant variation from one sample to the next. Given that C-C bonds are 3.65 eV, we cannot rule out that two different LO-type shallow defects may be contributing to breakdown if these results are to be taken at face value. As stated earlier, fitting step-up to breakdown data with physics-based equations is novel to the best of our knowledge. The product series used assumes that each step is statistically independent and thus neglects any aging (particularly changes in defect density).

Given the simplifying assumptions in the theory, we cannot expect the results to be exact, only indicative of the underlying physical mechanisms.

In Fig. 1, we note that for BOPP, PI 2008, PI 2017, and PEEK, the dual defect model gives essentially the same result as the Crine model. This is also evident in the similarities between the resulting defect energies and sometimes large uncertainties in fitting parameters displayed in Table I. Applying Occam's razor, we must conclude that, in these cases we cannot claim the dual-defect model provides any advantage over Crine's mean field approximation. In other words, this suggests that only one defect mechanism dominates for these materials in their corresponding test conditions. This is consistent with others' results for BOPP only showing bimodal behavior after significant thermal aging [16].

For LDPE and PI 2012-13, the dual-defect fit is clearly an improvement over the Crine model fit. In a previous publication we suggested that, for LDPE, that when a mixed Weibull fit is better than a single Weibull fit there must be two underlying defect modes consistent with our dual-defect model of breakdown [10]. In other words, when a mixed Weibull fit is better than a single Weibull fit, we would expect that the dual-defect model fit would be better than a Crine model fit; in LDPE

this is indeed the case. For PI 2012-2013 this is also true although the improvements are smaller. Fits to PI 2017 did not corroborate this conclusion, as the mixed Weibull is the best Weibull fit while both single and dual-defect physics-based models give essentially the same result. Nevertheless, visually we see that the data for PI 2008 and PI 2017 agree very well at higher fields while deviating at lower fields. This perhaps indicates that the two PI data sets exhibit the same deep defect mechanism but different shallow defects; this seems reasonable for two batches of the same material which are nominally the same. While the physics-model fits do not show this, the mixed Weibull fits are indicative of such behavior. Turning to PEEK, we see that there are not enough data to tell whether any bimodal behavior exists, even with Weibull distributions.

IV. CONCLUSIONS

Weibull fits to step-up data are simple and practical for comparing materials or test conditions. When mixed Weibull fits are better than single Weibull fits, this may indicate multiple underlying defect mechanisms; however, Weibull statistics do not offer any direct estimates of intrinsic material properties. Both single- and dual-defect model fits offer direct estimates of defect energies and densities. Except in one case—one of the three batches of PI—in this study, the dual-defect model is a better fit to bimodal distributions of tests results. Both Crine and dual-defect model fits offer estimates of trap energies and densities. Except in one case in this study, the dual-defect model results in a better fit to obviously bimodal data.

As spacecraft are exposed to more extreme charging environments there is an increasing need for better materials properties characterization, including the field-dependent distribution of breakdown strength. It is clear that relying on minimal number of tests is not enough to characterize a material well. While the dual-defect model we present is shown to be an improvement over a mean field theory in some cases, it is clear that further theoretical development is needed.

ACKNOWLEDGMENT

This work was supported by a NASA Space Technology Research Fellowship.

The research was carried out at Utah State University and the Jet Propulsion Laboratory, California Institute of Technology, under a contract with the National Aeronautics and Space Administration.

Copyright 2019. All rights reserved.

REFERENCES

- [1] R.D. Leach, and M. B. Alexander, "Failures and Anomalies Attributed to Spacecraft Charging," NASA Marshall Space Flight Center, 1995.
- [2] C. C. Reed, R. Briët, and M. Begert, "ESD Detection, Location and Mitigation, and Why they are Important for Satellite Development, 13th Spacecraft Charging Tech," in *Conf., (Pasadena, CA)*, 2014.
- [3] D. C. Ferguson, S. P. Worden, and D. E. Hastings, "The Space Weather Threat to Situational Awareness, Communications, and Positioning Systems," *Plasma Science, IEEE Transactions on*, vol. 43, no. 9, pp. 3086-3098, 2015.
- [4] *Mitigating in Space Charging Effects—A Guideline*, document NASA-HDBK-4002A, 2011.
- [5] H. B. Garrett and A. C. Whittlesey, *Guide to mitigating spacecraft charging effects*. John Wiley & Sons, 2012.
- [6] *Draft Standard on Spacecraft Charging: Environment-Induced Effects on the Electrostatic Behaviour of Space Systems*, document ECSS-E- ST-20-06C, 2003.
- [7] *Spacecraft Charging and Discharging*, document JAXA Paper JERG-2-211A, 2012.
- [8] W. Kim, J. Z. Chinn, I. Katz, H. B. Garrett, and K. F. Wong, "3-D NUMIT: A general 3-D internal charging code," *IEEE Transactions on Plasma Science*, vol. 45, no. 8, pp. 2298-2302, 2017.
- [9] A. Andersen, J. R. Dennison, and K. Moser, "Perspectives on the Distributions of ESD Breakdowns for Spacecraft Charging Applications," *IEEE Transactions on Plasma Science*, vol. 45, no. 8, pp. 2031-2035, 2017.
- [10] A. Andersen and J. R. Dennison, "Mixed Weibull distribution model of DC dielectric breakdowns with dual defect modes," in *Electrical Insulation and Dielectric Phenomena (CEIDP), 2015 IEEE Conference on*, 18-21 Oct. 2015 2015, pp. 570-573.
- [11] A. Andersen, "The Role of Recoverable and Non-recoverable Defects in DC Electrical Aging of Highly Disordered Insulating Materials," PhD, Department of Physics, Utah State University, Logan, UT, 2018.
- [12] A. Andersen, J. R. Dennison, A. M. Sim, and C. Sim, "Electrostatic Discharge and Endurance Time Measurements of Spacecraft Materials: A Defect-Driven Dynamic Model," presented at the 13th Spacecraft Charging Technology Conference, Pasadena, CA, 2014.
- [13] J.-P. Crine, J.-L. Parpal, and C. Dang, "A new approach to the electric aging of dielectrics," in *Electrical Insulation and Dielectric Phenomena, 1989. Annual Report., Conference on*, 1989: IEEE, pp. 161-167.
- [14] A. Andersen, J. R. Dennison, A. M. Sim, and C. Sim, "Measurements of Endurance Time for Electrostatic Discharge of Spacecraft Materials: A Defect-Driven Dynamic Model," *Plasma Science, IEEE Transactions on*, vol. 43, no. 9, pp. 2941-2953, 2015.
- [15] *Standard Test Method for Dielectric Breakdown Voltage and Dielectric Strength of Solid Electrical Insulating Materials Under Direct-Voltage Stress*, ASTM, 2014.
- [16] M. Ritamäki, I. Rytöluoto, K. Lahti, T. Vestberg, S. Pasanen, and T. Flyktman, "Large-area approach to evaluate DC electro-thermal ageing behavior of BOPP thin films for capacitor insulation systems," *IEEE Transactions on Dielectrics and Electrical Insulation*, vol. 24, no. 2, pp. 826-836, 2017.